

Real-Time Stereo 3D Ultrasound

JOANNA R. NOBLE, MATTHEW P. FRONHEISER AND STEPHEN W. SMITH

*Department of Biomedical Engineering
Duke University
Durham, NC 27708
ssmith@duke.edu*

Real-time 3D ultrasound was developed at Duke University in 1991 and has since been used with a variety of transducers and shown effectiveness in clinical applications and *in vivo* animal imaging studies. Methods for displaying the 3D pyramid of data acquired by the system include selecting 2D image slices or integrating data into a volume rendered view. A third method, real-time stereo 3D imaging, is discussed here. The clinical commercial 3D system has been modified in our laboratory to display a real-time stereo image pair on the scanner display to be viewed through a stereoscope. This merges the pair into a single image, with a sensation of depth. Stereoscopic displays have previously been demonstrated to provide benefits, including improved depth judgments and increased perception of image quality in other applications. Previously-saved volumes of ultrasound data are shown in stereo 3D using the new system.

Key words: Stereo display; two-dimensional array; volumetric imaging.

I. INTRODUCTION

Real-time 3D ultrasound using a 2-D array transducer was developed at Duke University and described by Smith et al and von Ramm et al^{1,2} in 1991. The system was commercialized by Volumetrics Medical Imaging, Inc. (VMI), Durham, NC. The Duke/VMI scanner uses a matrix-array transducer with up to 512 active channels and 16:1 receive mode parallel processing to generate 3D pyramidal scans at up to 30 volumes/sec (Fig. 1a). The original Duke/VMI scanner used a 2.5 MHz or 3.5 MHz transthoracic transducer, also commercialized by VMI.³ The scanner has since been adapted for use with other transducers, including transesophageal,⁴ laparoscopic⁵ and catheter transducers at 5, 7, 10 and 15 MHz⁵⁻⁷ with as many as $256 \times 256 = 65,536$ elements and 512 active channels.^{8,9} The Duke/VMI scanner has shown effectiveness in clinical and animal assessments of applications including measurement of left-ventricular volumes,¹⁰ detection of perfusion defects,¹¹ decreased scan time compared to 2D scanners for recognition of dobutamine-induced ischemia,¹¹ improved depiction compared to 2D scanners of distribution of spatial velocity in the left ventricular out-flow track,¹³ improved imaging compared to fluoroscopy for placement of bioptomes in the right ventricle¹⁴ and detection of congenital cardiac defects.¹⁵ More recently, real-time 3D systems have become widely commercialized for obstetric, cardiac and radiologic applications.

Two methods have been previously developed for the Duke/VMI scanner to display the 3D volume of ultrasound data on the 2D monitor. The first method displays 2D slices from the volume, i.e., two 'B-scans,' slices of image data orthogonal to each other and to the transducer face and two or three 'C-scans,' slices of image data parallel to the transducer face. The

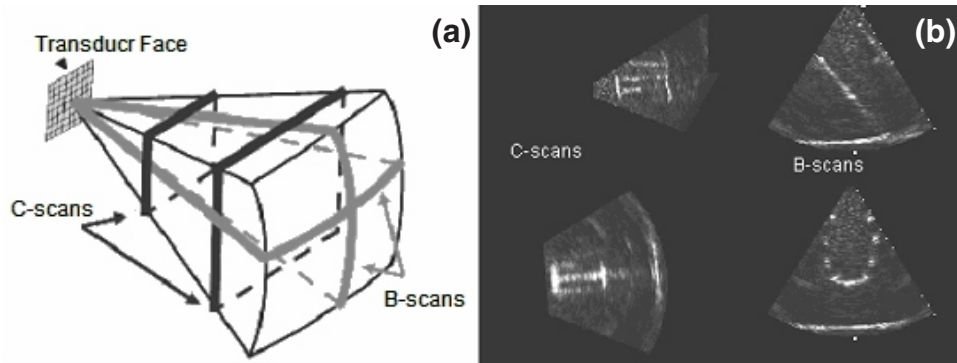


FIG. 1 2D B-scan and C-scan slices method of display for 3D ultrasound: (a) Schematic for array transducer and captured volume of data, with B-scan and C-scan image planes darkened. (b) Example of Duke/VMI ultrasound display screen that simultaneously shows C-scans in the left column and B-scans in the right column

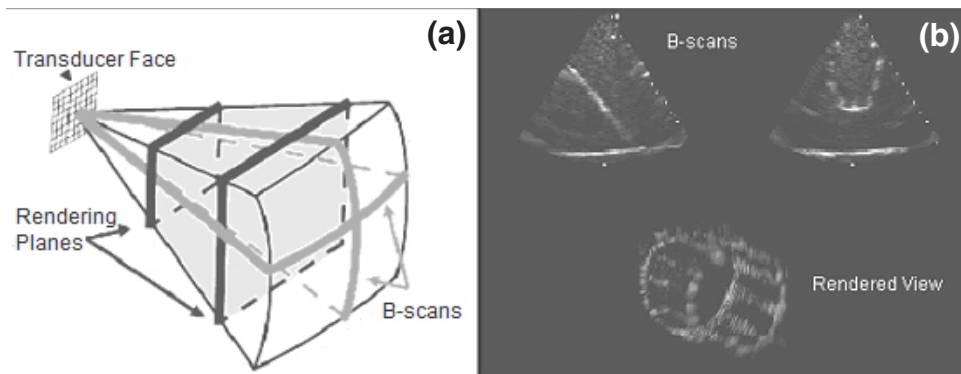


FIG. 2 Volume rendering method of display for 3D ultrasound: (a) Schematic for array transducer and captured volume of data with B-scan slices and the rendered volume darkened. (b) Example of Duke/VMI display screen that simultaneously shows B-scans in the top row and a volume-rendered thick slice below.

angle between the B-scan and transducer face is user-controlled such that the B-scan slice can sweep through the complete 65° - 120° pyramidal volume, as selected by the user. The C-scans also can be rotated up to a full 180° from their initial parallel position and the C-scan depth can be adjusted to any level in the volume of data. The spacing between the C-scans and thickness of the slices can also be varied. The C-scans are linked together such that their angles are varied simultaneously and cannot differ from each other. The monitor then displays the two or three C-scans in a vertical column on the left-hand side and the two B-scans in a column on the right-hand side. Figure 1b illustrates the relationship between the captured volume and this type of display:

The second display method, volume rendering, also displays the B-scan slices. However, instead of displaying the C-scans as individual slices, the user selects the C-scan spacing and the information between the two indicated depths is integrated and spatially filtered to be displayed as one thick volume-rendered C-scan. The B-scan angle, volume-rendered image angle and depth can be varied just as for the first method. Figure 2 shows the volume-rendering method used to image a metal cage.

This paper discusses a third method of displaying the 3D volume of data on the ultrasound monitor: real-time stereo 3D imaging. Stereo vision is largely responsible for human depth perception. Because the eyes are separated by a horizontal distance, the left and the right eye

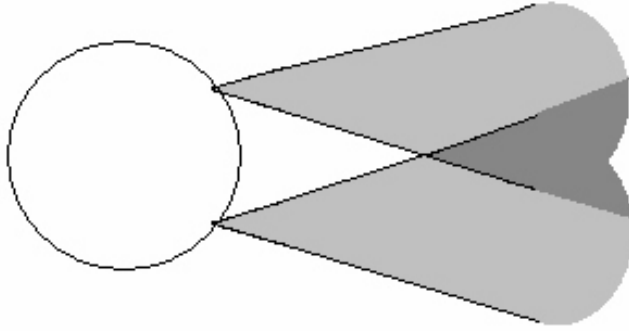


FIG. 3 Stereo vision: left and right eyes view the same scene from different angles.

receive slightly different perspectives of the same scenery. The brain processes these differences to find depth information and create a 3D stereo image.¹⁶

Figure 3 illustrates the perspectives of the left eye versus the right eye.

This type of depth perception is not possible in a single 2D image because the image is taken from a single perspective and all of the objects are in the plane of the image. Stereo image pairs are images taken of the same object, from different orientations to mimic the left eye and right eye views. Specialized viewing techniques or a stereoscope can then be used to merge these two images and gain a 3D effect. The technique of stereo image pairs is generally used with photography but has been applied to ultrasound to develop a display that presents two adjacent scans, taken from the same depth and rotated from each other, mimicking a natural subtended angle for the left and right eyes. The observer's defocused eyes or a stereoscope can then be used to merge these two images and gain a 3D effect.

The benefits of stereoscopic displays for a variety of uses have been discussed numerous times and include improved depth judgments and an increase in an individuals' perceptions of image quality.^{17,18} The possibility of real-time stereo 3D ultrasound was first introduced by our lab at Duke² in 1991 in the form of images rotated 7° from each other by using two video cameras as a scan converter. In 1995, Martin, et al outlined a system employing electronic shutter glasses to view stereo pairs of 3D echocardiographic ultrasound images (rotated 5° from each other) and showed that this method improved capabilities for distinguishing separateness of distinct 3D structures.¹⁹ In 1996, State et al described a head-mounted display combining standard 2D display of ultrasound data with stereo images from two head-mounted video cameras that enabled a physician to guide a needle into a model tumor inside a phantom of a human breast with ease.²⁰ In 2005, Huang et al detailed a system that makes simultaneous use of two ultrasound transducers rotated 21-45° from each other to directly create stereo image pairs in real-time.²¹ Most recently, Novotny et al have performed a series of trials comparing 2D displays of 3D ultrasound to optical endoscope displays and to 3D ultrasound rendered in combination with stereoscopic video images in electronic shutter glasses. The trials evaluated user-controlled robot manipulation tasks and showed the stereo/3D ultrasound combination facilitated guidance better than the 3D ultrasound but not as well as the endoscope.²²

To our knowledge, this paper describes the first real-time display of stereo image pairs from 3D volumes of ultrasound data on a clinical scanner monitor by software modifications of the scanner's scan converter. The position of the transducer, the depth of the scan and the angle of the scan can all be adjusted without interfering with the stereo feature. Moreover, no additional hardware is required to achieve this stereo display other than a stereoscope for merging the stereo pair into a 3D image required by some human observers.

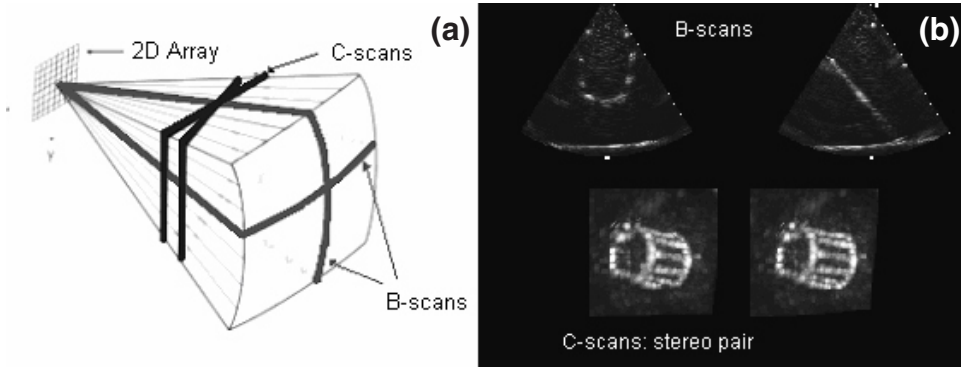


FIG. 4 Stereo image pair method of display for 3D ultrasound: (a) Schematic for array transducer and captured volume of data, with B-scan and C-scan image planes darkened. (b) Example of Duke/VMI ultrasound display screen that simultaneously shows stereo pair of C-scans below the standard B-scans.

This paper provides examples of stereo displays using ultrasound data from previously-saved video volumes using a variety of 3D transducers, including a transthoracic probe, transesophageal echocardiography probe, 3D brain endoscope and a dual lumen intracardiac catheter probe.

II. METHODS

Stereo ultrasound system

The implemented stereo 3D technique places the tilted stereo images side-by-side so that the user can merge the pair by defocusing his eyes or via a stereoscope. The relationship between the volume of data and display is similar to that in the slice method discussed in the introduction. The B-scan angle, C-scan angle, C-scan depth and C-scan thickness may all be varied. The two C-scans are tilted 7° from each other at the touch of a button. Our observer studies showed this angle to be the most comfortably viewed for images using the Duke/VMI scanner. Figure 4 illustrates the association between the captured volume (Fig. 4a) and the display (Fig. 4b), analogous to figures 1 and 2.

The C-scans on the screen and on the pages of this paper can be merged by allowing the eyes to diverge (i.e., focus at infinity) or by viewing the screen through a stereoscope. A stereoscope schematic, shown in figure 5, uses mirrors to present the eyes with two different images as though they are originating from the same location. This causes the eyes to naturally merge the image pair. Our system used a ScreenScope Mirror Stereoscope (Stereo Aids, Albany, AU) for attaching to a computer monitor.

The sensation of depth was found to increase with C-scan slice thickness; so the system software was modified to enable C-scans up to 4 cm thick. As the C-scan is tilted farther from parallel, the two slices displayed by the two angles begin to differ in size and shape. This caused ghosting when the pair was viewed through the stereoscope. To aid in merging, the C-scan windows on the screen were reduced to crop the two images to the same size.

Stereo pairs of saved volumes

Six different previously-saved volume segments of ultrasound data were loaded into the Duke/VMI scanner and viewed with the stereo 3D method. Many of these volumes were saved from *in vivo* animal studies, displaying the dynamic imaging capability of stereo 3D ultrasound in a tissue environment.

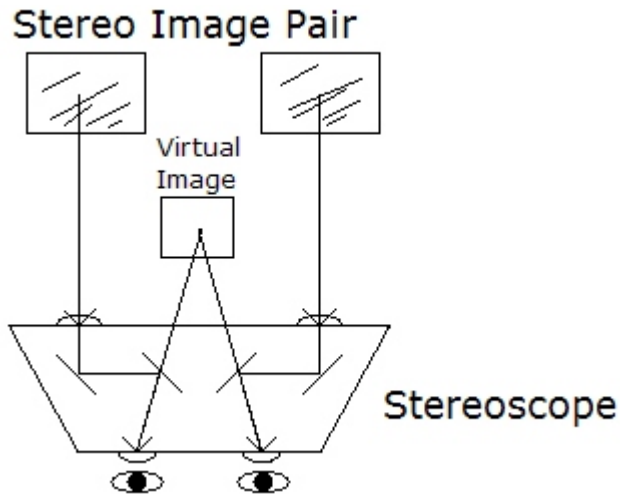


FIG. 5 Stereoscope diagram: Each eye is presented with a different image simultaneously, causing the image pair to merge into a single perceived image.

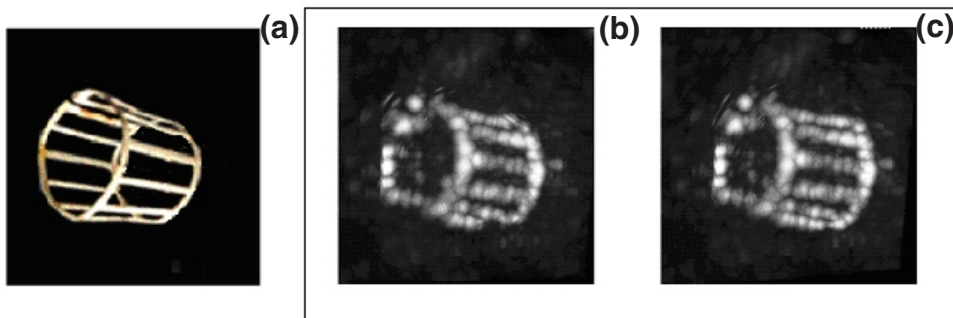


FIG. 6 Metal cage: (a) Photograph. (b) Stereo image pair made using transthoracic probe

III. RESULTS

Figure 6b shows a small metal cage that was suspended in a tank of water while a volume of data was captured using the 2.5 MHz transthoracic probe with the Duke/VMI scanner. Figure 6a shows a photograph of the cage for comparison.

Figure 7 shows a mitral valve imaged during an *in vivo* canine study. A 5 MHz probe with 504 active channels, developed for transesophageal echocardiography (TEE), was used. This probe is described in a 2004 article by Pua, et al.⁴

Figure 8 shows a needle inside of the esophagus also captured using the TEE probe during an *in vivo* canine study.

Figure 9 shows an Amplatzer[®] occluder (AGA Medical Corp. Golden Valley, MN), again imaged in a tank of water with the TEE probe. The occluder is a self-expandable disk consisting of wire mesh and polyester fabric. It is used to repair the heart without open-heart surgery because it can be delivered to the heart through blood vessels.²³

Figure 10 shows a needle near the lateral ventricles of the brain, captured using a forward viewing 3D ultrasound endoscope equipped with an accessory port during an *in vivo* canine study in which the brain was imaged in a coronal view through a 1 cm burr hole in the skull.²⁴

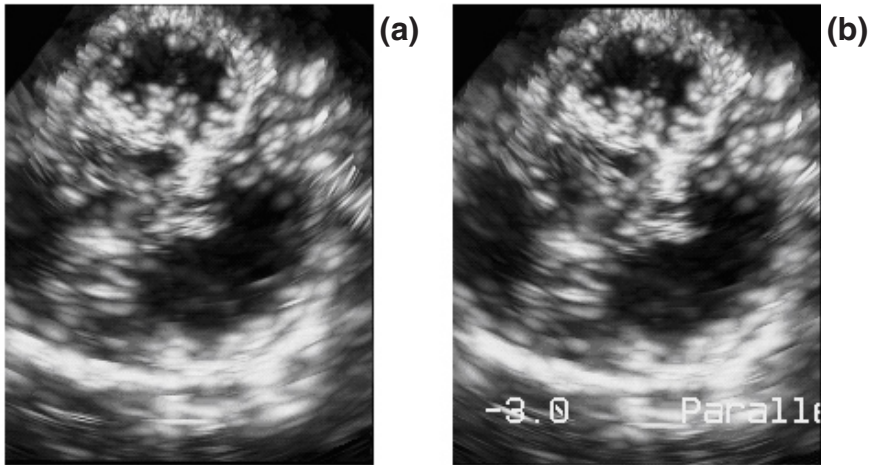


FIG. 7 Stereo image pair of canine mitral valve using a transesophageal echocardiography probe.

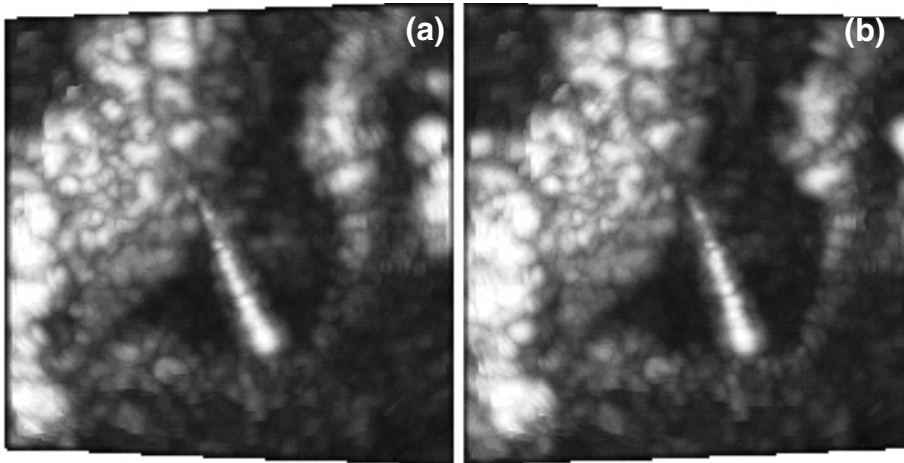


FIG. 8 Stereo image pair of needle in canine esophagus imaged using TEE probe

Figure 11 displays a 0.36 mm diameter guidewire inserted into the coronary sinus imaged using a forward-scanning dual-lumen 3D catheter probe during an *in vivo* sheep study. For this image, the guidewire traveled through the working lumen of the catheter. The probe was operating at 5 MHz with 112 active channels.²⁵

IV. DISCUSSION

The new stereo system makes it possible to view stereo pairs of images of the ultrasound data in real-time by viewing the data from volumetric scans simultaneously from different angles. The addition of the stereoscope allows any user to easily merge the images. For distinctly-imaged objects, such as those pictured in figures 6-9, the stereo 3D adds a greater depth sensation and increases the visual appeal. For less distinctly-imaged objects, the stereo 3D makes it easier to differentiate the components. For instance, in figure 10, the needle becomes easily distinguishable from the tissue when the images are merged.

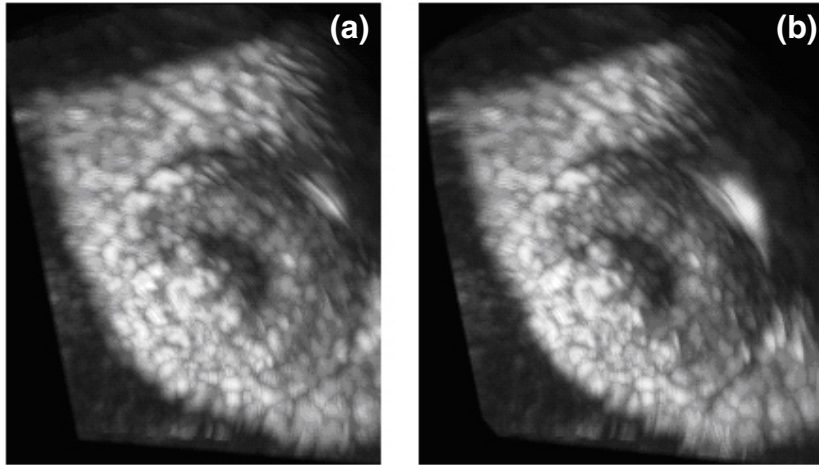


FIG. 9 Stereo image pair of Amplatzer® occluder imaged using TEE probe

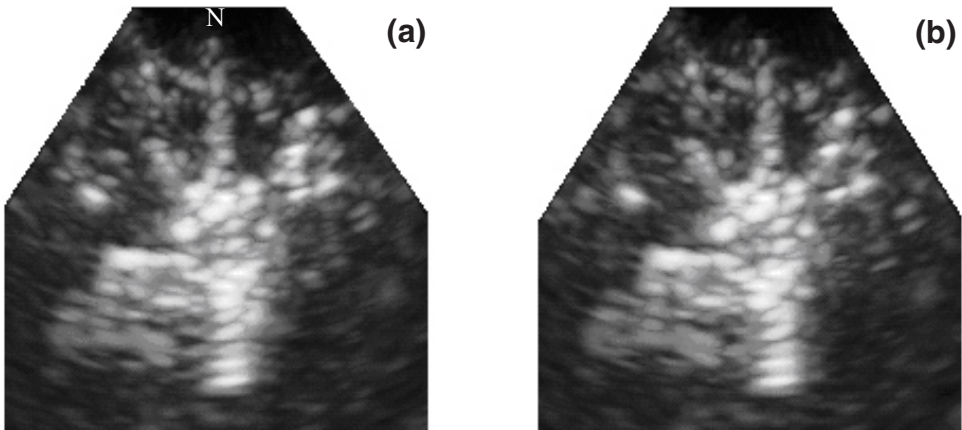


FIG. 10 Stereo image pair of needle (N) in canine brain imaged using 3D ultrasound endoscope.

In order to implement the stereo 3D, some incidental alterations were made to the system, as described previously, which may also have affected the effectiveness of the method and any comparison to the other methods for displaying a volume of data. For example, the maximum allowable C-scan thickness was increased based on the conjecture that stereo 3D would be more useful for viewing an image containing data at a greater range of depths. This actually provided a more information-rich picture for both merged and unmerged images. In addition, the display was changed to label the angle of the C-scan plane from parallel, in addition to the angles of the B-scan planes from orthogonal. This was useful for recording the best scan plane locations to view a given volume of image data.

Some of the alterations subtracted from the overall usefulness of the system. The necessity of cropping the C-scans to prevent ghosting caused loss of information imaged at the edges of the C-scans. Moreover, maintaining a C-scan spacing of zero removed the capacity of the system to simultaneously display C-scan data at different depths. Additionally, the B-scans became distorted when viewed through the stereoscope. Therefore, to switch from viewing the merged C-scans and the nonstereoscopic B-scans, the user had to remove his head momentarily from the stereoscope.

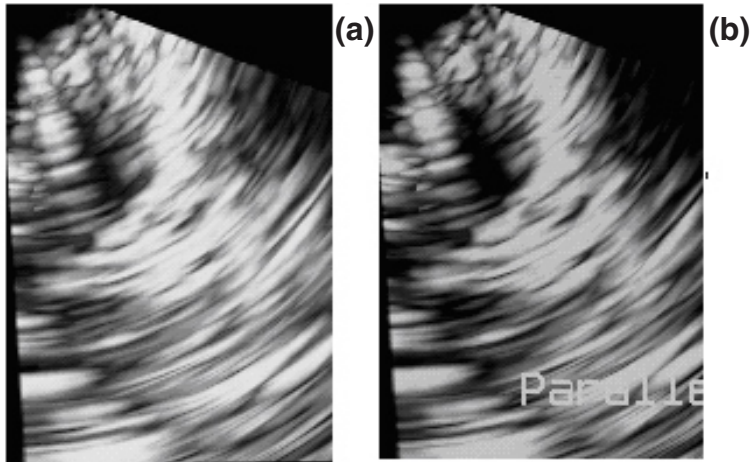


FIG. 11 Stereo image pair of guidewire in the sheep coronary sinus imaged using dual-lumen 3D catheter

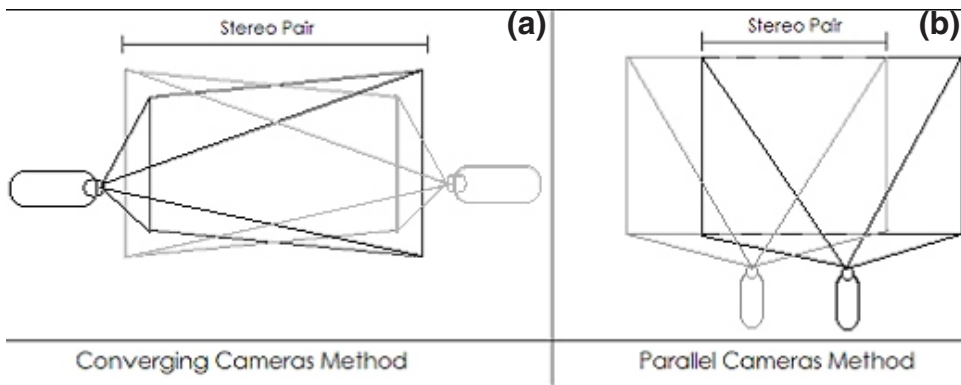


FIG. 12 Methods for creating a stereo pair: (a) Converging Cameras causes vertical parallax in the corners. (b) Parallel Cameras creates a stereo pair from the overlapping views

There are more sophisticated stereo display techniques that may enhance perception. To create our stereo image pairs, the two displayed slices were tilted away from each other along a central axis, as illustrated in figure 4. This technique of stereo 3D uses two converging views to record a scene. Alternatively, photographers employ parallel cameras directed straight ahead to capture overlapping sections that can be used as stereo pairs. The two methods are illustrated in figure 12:

As shown in figure 12a, when using the converging cameras method, the image in each camera appears larger on one side than the other. The larger side is switched between the two cameras, resulting in a vertical difference between the images that increases towards the corners. This difference is known as ‘keystone distortion’ in photography and is eliminated by using the parallel cameras method.²⁷ Figure 4 shows that a similar distortion occurs with the current method of stereo 3D ultrasound. For each C-scan, the side farther from the transducer is larger, (the opposite occurs in photography), causing vertical distortion in the corners of the merged image. However, both the converging cameras methods and parallel cameras method create the sensation of 3D, and the pyramid of data was more easily adapted to the converging cameras method. Implementing the parallel camera method for ultrasound scanning would require multiple ultrasound scanners, transducers or multiplexing, which would reduce speed and dramatically increase complexity.

ACKNOWLEDGMENTS

The authors would like to thank Eric C. Pua and Edward D. Light and Timothy Shih for their assistance on this project. This work was supported in part by NIH grants HL-64962 and HL-72840.

REFERENCES

1. Smith SW, Pavy HG, von Ramm OT. High speed ultrasound volumetric imaging system part I: transducer design and beam steering, *IEEE Trans Ultrason Ferroelectr Freq Contr* 38, 100-108 (1991).
2. von Ramm OT, Smith SW, Pavy HG. High speed ultrasound volumetric imaging system part II: parallel processing and image display, *IEEE Trans Ultrason Ferroelectr Freq Contr* 38, 109-115 (1991).
3. Light ED, Davidsen RE, Fiering JO, et al. Progress in two-dimensional arrays for real-time volumetric imaging, *Ultrasonic Imaging* 20, 1-15 (1998).
4. Pua EC, Idriss SF, Wolf PD, Smith SW. Real-time 3D transesophageal echocardiography, *Ultrasonic Imaging* 26, 217-232 (2004).
5. Light ED, Idriss SF, Sullivan KF, et al. Real-time 3D laparoscopic ultrasonography, *Ultrasonic Imaging* 27, 129-144 (2005).
6. Lee W, Idriss SF, Wolf PD, Smith SW. A miniaturized catheter 2-D array for real-time, 3-D intracardiac echocardiography, *IEEE Trans Ultrason Ferroelectr Freq Contr* 51, 1334-1346 (2004).
7. Light ED, Smith SW. Two dimensional arrays for real time 3D intravascular ultrasound, *Ultrasonic Imaging* 26, 115-128 (2004).
8. Yen JT, Smith SW. Real-time rectilinear volumetric imaging, *IEEE Trans Ultrason Ferroelectr Freq Contr* 49, 114-124 (2002).
9. Yen JT, Smith SW. Real-time rectilinear 3-D ultrasound using receive mode multiplexing, *IEEE Trans Ultrason Ferroelectr Freq Contr* 51, 216-226 (2004).
10. Schmidt MA, Ohazama CJ, Agyeman KO, et al. Real-time three-dimensional echocardiography for measurement of left ventricular volumes, *Am J Cardiol* 84, 1434-1439 (1999).
11. Camarano G, Jones M, Freidlin RZ, Panza JA. Qualitative assessment of left ventricular perfusion defects using real-time three-dimensional myocardial contrast echocardiography, *J Am Soc Echocardiogr* 15, 206-213 (2002).
12. Ahmad M, Tianrong X, McCulloch M, et al. Real-time three-dimensional dobutamine stress echocardiography in assessment of ischemia: comparison with two-dimensional dobutamine stress echocardiography, *J Am Coll Cardiol* 37, 1304-1309 (2001).
13. Tsujino H, Jones M, Shiota T, et al. Real-time three-dimensional color doppler echocardiography for characterizing the spatial velocity distribution and quantifying the peak flow rate in the left ventricular outflow tract, *Ultrasound Med Biol* 27, 69-74 (2001).
14. McCreery CJ, McCulloch M, Ahmad M, deFilippi CR. Real-time 3-dimensional echocardiography imaging for right ventricular endomyocardial biopsy: a comparison with flurosocopy, *J Am Soc Echocardiogr* 14, 927-933 (2001).
15. Fleishman CE, Li J, Ota T, et al. Identification of congenital heart defects using real time three-dimensional echo in pediatric patients, *Circulation* 94, 2423 (1996).
16. Diner DB, Fender DH. *Human Engineering in Stereoscopic Viewing Devices*, pp. 3-19 (Plenum Press, New York, 1993).
17. Jones G, Lee D, Holliman N, Ezra D. Controlling perceived depth in stereoscopic images, in *Proc SPIE Stereoscopic Displays Virt Reality Syst VIII* 4297, pp. 42-53 (2001).
18. Reinhart WF, Beaton RJ, Snyder HL. Comparison of depth cues for relative depth judgments, in *Proc SPIE Stereoscopic Displays Appl* 1256, pp. 12-21 (1990).
19. Martin RW, Legget M, McDonald J, et al. Stereographic viewing of 3D ultrasound images: a novelty or a tool?, in *Proc IEEE Ultrason Symp* 2, pp. 1431-1434 (1995).

20. State A, Livingston MA, Garrett WF, et al. Technologies for augmented reality systems: realizing ultrasound-guided needle biopsies, in *Conf Proc Comput Graph Interact Tech*, pp. 439-446 (1995).
21. Huang C, Auner GW, Caulfield HJ, Rather JDG. Three-dimensional ultrasound imaging, *Acoust Res Lett Online* 6, 53-57 (2005).
22. Novotny PM, Kettler DT, Jordan P, et al. Stereo display of 3D ultrasound images for surgical robot guidance, in *Int Conf Proc IEEE Eng Med Biol Soc*, pp. 1509-1512 (2006).
23. New device approval: Amplatzer® septal occluder - p000039, U.S. Food and Drug Administration Center for Devices and Radiological Health Consumer Information, <http://www.fda.gov/cdrh/mda/docs/p000039.html> (Up24. Light ED, Mukundan S, Wolf PD, Smith SW. Real-time 3D intracranial ultrasound, *Ultrasound Med Biol* (accepted for publication).
25. Lee W, Idriss SF, Wolf PD, Smith SW. Dual lumen transducer probes for real-time 3-D interventional cardiac ultrasound, *Ultrasound Med Biol* 29, 1297-1304 (2003).
26. Ijsselstein WA, de Ridder H, Vliegen J. Subjective evaluation of stereoscopic images: effects of camera parameters and display duration, *IEEE Trans Circ Syst Video Tech* 10, 225-233 (2000).
27. Woods A, Docherty T, Koch R. Image distortions in stereoscopic video systems, in *Proc SPIE Stereoscopic Displays Appl IV 1915*, pp. 1-13 (1993).